# Critical Temperature of Polished $TmVO_4$ Sample as a Function of the c-field

Tianna Green
*Physics Department, University of California Davis*

$TmVO_4$ experiences a structural phase transition from tetragonal ($C_4$) to orthogonal ($C_2$) below 2.15K and has garnered interest because it exhibits Ising nematic ordering without competing phases, unlike other materials such as the iron pnictide superconductors [1]. We performed $^{51}$V Nuclear Magnetic Resonance (NMR) at 1.35T to probe the local nuclear environment as the thulium (Tm) ions exhibit ferroquadrupolar ordering due to Jahn-Teller distortion with a non-Kramers ground state doublet. A polished sample was utilized to decrease previously recorded peak broadening as a result of demagnetization field inhomogeneity. Experimental data suggests the critical temperature ($T_Q$) for this phase transition decreases as a function of the magnetic field along the c-axis, as the sample approaches the quantum critical point (QCP).

## I. INTRODUCTION

Rare earth vanadates and arsenates of thulium (Tm) exhibit several favorable properties that prompt investigation into phase transitions caused by the co-operative Jahn-Teller effect (CJTE). The CJTE is a phase transition between the electronic states and lattice vibrations and includes the transformation of the crystal lattice to a lower-level symmetry [2]. In the case of $TmVO_4$ **[Fig 1]** below 2.15K, the Tm electron orbitals in the $4f^{12}$ state (S = 1, L = 5, J = 6) spontaneously align, breaking the $C_4$ symmetry of the crystal and reducing it to $C_2$.

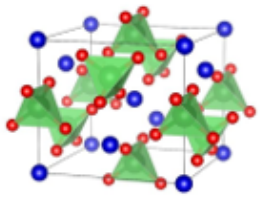

FIG. 1: Unit cell of $TmVO_4$ ($C_4$ symmetry). Tm ions represented in blue, V is within the green pyramids bonded to the red O molecules.

The ground state of the Tm ion is a non-Kramer's doublet, which inhibits it from magnetic ordering. Instead, as we approach $T_Q$ the electron orbitals form a strong coupling to the crystal lattice and the quadrupole moments interact and align. This phenomenon is known as ferroquadrupolar ordering and breaks the same symmetries as Ising nematic ordering, thus, can be used to understand the latter phase transition [4,7]. In addition to modeling Ising nematic ordering, the relatively low critical temperature and symmetry of $TmVO_4$ allows us to analyze the phase transition without the need to isolate it from other thermal effects [2]. Because it is an insulator, $TmVO_4$ bypasses the superconductivity phase often observed in conductors at low temperatures, giving easier access to approach the QCP and detect long-range quantum criticality effects. For the above reasons, studying the nematic fluctuations of $TmVO_4$ is invaluable.

## II. BACKGROUND

### NMR

Nuclear spin, I, is the intrinsic angular momentum of nuclei. Spin is quantized as 1/2 integer values (S = 0, 1/2, 1, 3/2, 2,...etc), and as later discussed, $TmVO_4$ is I = 7/2. To perform NMR, one needs an isotope with a nonzero spin that occurs with sufficiently high natural abundance to perform measurements. Nearly every element has at least one isotope with nuclear spin, making NMR an ideal tool to explore the physical and chemical properties of materials through examining the local environment of the nuclei.

### A Classical Approach

Nuclei with spin also have an associated magnetic moment that is at the heart of NMR. It is helpful to think of these magnetic moments as arrows that indicate their orientation with respect to each other and/or a magnetic field (**H**). In the absence of an external magnetic field ($H_0$ along the z-axis), the nuclear spins point randomly. Once an external magnetic field is introduced two things happen: the nuclear spins begin to precess about $H_0$ and a net magnetization vector is created. The precession of the nuclei is given by the Larmor frequency: $f = \gamma H_0$, where the gyromagnetic ratio ($\gamma$) is the ratio between the magnetic moment and angular momentum of the nucleus **[Fig 2]**. For $^{51}$V, $\gamma$ = 11.193 MHz/T and we chose $H_0$ = 1.35T, therefore $f$ = 15.1065MHz. Contrary to what many textbooks incorrectly portray, nuclear spins do not align parallel or antiparallel to $H_0$. Rather, spins populate the quantized energy levels according to the Boltzman distribution, and produce a net magnetization vector (***M***) that lies parallel to $H_0$ **[Fig 3]**. Although not inherently intuitive by any means, this concept is analogous to putting several compasses in a dryer (assuming they remain undamaged for the sake of this argument). While the compasses will prefer to align north to Earth's gravitational field, they are not given a chance to as they bounce off the dryer walls and each other, however at any given moment the net alignment will point north [7]. Likewise, nuclear orientations fluctuate due to magnetic interactions, yet in the presence of an external magnetic field will bias towards it. **M** can be perturbed from thermal equilibrium to precess

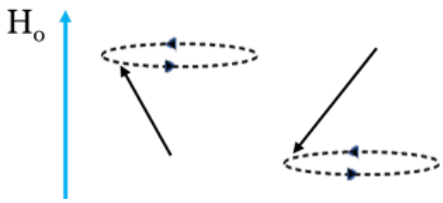


FIG. 2: In an external magnetic field ($H_0$), nuclei precess like a top about $H_0$. Not all the nuclei are at the same angle from $H_0$, which is indicated in the above example showing how the precession would work for two sample angles.

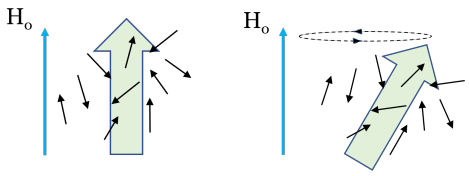


FIG. 3: In the presence of $H_0$, a magnetization vector, represented by the green arrow, forms parallel to $H_0$. Once a pulse is applied, the magnetization vector precesses in the transverse plane at the Larmor frequency.

around $H_0$. A radio frequency (RF) pulsed resonant with the Larmor frequency and polarized perpendicular to $H_0$ is utilized to begin this precession. An RF pulse can rotate **M** any amount from its equilibrium position. After applying an RF pulse, **M** precesses in the transverse plane at the Larmor frequency **[Fig 3]**. Specific pulse-sequences can be utilized to maximize signal measurements, such as the inversion recovery pulse utilized in this experiment. Prior to an RF pulse, **M** is stationary while the individual nuclei continue to precess. Conventionally, this is written as $M_z = M_0$ where $M_z$ denotes the z-component of **M** and $M_0$ is the equilibrium value of **M**. At any point where $M_z \neq M_0$, $M_z$ will approach $M_0$ exponentially with a time constant, $T_1$. $T_1$ is called the spin-lattice, longitudinal-, or thermal-relaxation time and depends on the thermal interactions and electronic structure of the sample [8]. Note that an RF pulse affects each of the relative orientations of the individual spins, which then collectively rotate as a unit that precesses coherently [7]. The transverse component of **M**, denoted $M_{xy}$, also has a relaxation time called $T_2$. $T_2$ is called the spin-spin or transverse-relaxation time and stems from the energy exchange with local environment, local magnetic field inhomogeneity, and nuclear interactions [8]. In a perfect world each individual nucleus would precess at the exact same frequency and $H_0$ is homogenous throughout the sample. Recall the precession of nuclei in an external magnetic field is $f = \gamma H_0$. Nuclei in a nonuniform magnetic field where $\mathbf{H} \neq H_0$, perhaps due to a slightly different local magnetic field, will no longer precess at the same frequency of nuclei in other parts of the sample. The net result is that the collective magnetization loses coherence over a time scale known as $T_2$. Therefore, $T_2$ is the time constant by which $M_{xy}$ decays or dephases. $T_1$ and $T_2$ characterize the behavior of the magnetization as:

$$M_z(t) = M_0(1 - e^{-t/T_1})$$

$$M_{xy}(t) = M_0 e^{-t/T_2}$$

Where $M_0$ represents the equilibrium magnetization and t is the time after an initialization pulse sequence.

### Signal

The actual signal that is measured to find $T_1$ and $T_2$ is a result of the precession of **M**. As **M** precesses, it generates an oscillating magnetic field. NMR takes advantage of this oscillating magnetic field by placing the sample in a solenoid oriented in the xy-plane, therefore inducing a voltage signal (Faraday's Law) as **M** relaxes to its equilibrium position. The signal decays over time because as $M_z$ approaches $M_0$, $M_{xy}$ will tend to zero. The time dependence of $M_{xy}$ produces the signal called the free induction decay (FID). A Fourier transform of the FID signal reveals an NMR spectrum as of intensity (a.u.) as a function of frequency (Hz).

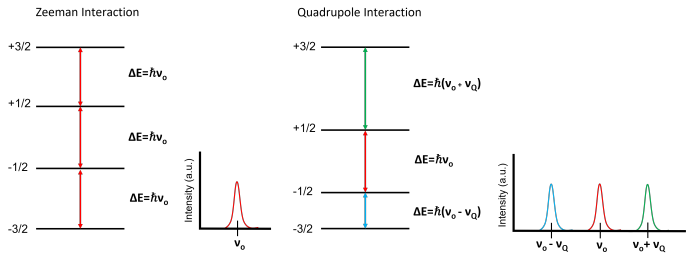


FIG. 4: In the case of I = 3/2, if only the Zeeman interaction is present, the energy levels are split evenly, therefore one peak is shown on an NMR spectrum. With the quadrupole interaction, the energy levels are no longer degenerate and 3 peaks are shown on the NMR spectrum separated by $\nu_Q$.

### A Quantum Sidenote

Classically, NMR can be explained with the discussion above. Quantum mechanics also plays a role in the actual signals that reveal the physical and chemical properties of the sample. Consider the simple case of a nucleus with spin 1/2. When $H_0 = 0$, the energy levels* are said to be degenerate, so only one energy level exists. When $H_0 \neq 0$, the energy level splits into 2 energy levels. In general, the number of energy levels is given by 2(I) + 1. This is called Zeeman splitting and the difference between the energy levels is $\Delta E = \hbar\nu_0$, where $\hbar$ is Planck's constant and $\nu_0$ is frequency (in this case $\nu_0$ = Larmor frequency). Therefore, the resonance spectrum would only show one peak at $\nu_0$. Moving on to a more complicated case, now consider a nucleus where I = 3/2, we will have 4 energy levels. If only the Zeeman interaction is present, the energy levels also split with a difference $\Delta E = \hbar\nu_0$, and still only one peak is observed**[Fig 4]**. This is not reality, however, due to the quadruple moment. In nuclei with I>1/2, a

quadruple moment due to a nonuniform internal distribution of charge occurs and causes a quadrupolar interaction. Due to quadrupolar interactions, the energy levels are no longer split evenly and are separated by an additional factor, $\nu_Q$, the nuclear quadruple frequency. The resonance spectrum now depicts three peaks at each resonance frequency **[Fig 4]**. In the case of $TmVO_4$, I = 7/2, therefore the NMR spectrum contains seven peaks separated by the nuclear quadruple frequency. *also known as eigenvalues or spin states.

## III. EXPERIMENT

### Sample

$TmVO_4$ was grown by collaborators at Stanford from $Pb_2V_2O_7$ with a 4 mol % of $Tm_2O_3$ [9]. The as-grown crystals were attached to a small cube using crystal bond and the sample corners and edges were polished using sanding paper into an ellipsoidal morphology to perform $^{51}$V NMR **[Fig 5]**. Earlier analysis of $TmVO_4$ revealed the rectangular sample acquires a nonuniform internal magnetic field (B) along the edges when exposed to an applied magnetic field ($H_0$) [5]. Immersing the sample in $H_0$ induces a magnetization (**M**), magnetic dipole per unit volume, that is given by M = $\chi H_0$, where  is the magnetic susceptibility. The demagnetization field ($H_d$) is created by the magnetic dipoles of the sample and opposes **M**, thus changing the magnetic flux density given by B = $\mu_0(H_d$ + M) [6]. The size and direction of $H_d$, depends critically on the position within the sample as well as the sample shape. For example, in a sphere or ellipsoid, $H_d$ is uniform, but for a cube or rectangular prism, $H_d$ is different at the edges and corners. Decreasing the demagnetization effects was imperative due to the significant line broadening and indistinguishable peaks observed with the original sample. Through polishing the sample, therefore reducing the edges, we have created an ellipsoid-like shape, resulting in a more homogeneous demagnetization. Due to these efforts, we now observe seven distinct peaks at low field, low temperature measurements.

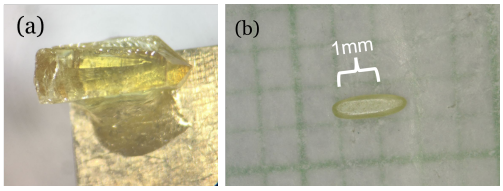


FIG. 5: (a) An unpolished 5% Y-doped $TmVO_4$ sample. The unpolished pure $TmVO_4$ sample would look similar. (b) The polished $TmVO_4$ sample used in the experiment.

### Experiment Setup

After measuring the dimensions, a copper coil was made to hold the sample. To ensure the sample did not rotate in the coil, it was secured with epoxy to a plastic platform. This platform was then soldered onto an LC circuit attached to a cryogenic goniometer NMR probe that would allow the crystal to rotate with manual input at precise angles **[Fig 6]**. The

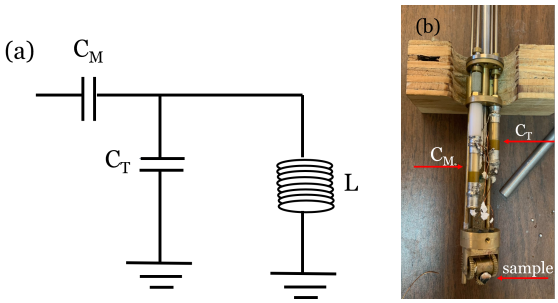


FIG. 6: (a) A circuit diagram of the LC circuit used. (b) The probe with a mounted sample. The two capacitors are labeled: $C_T$ is the tuning capacitor and $C_M$ is the matching capacitor.

probe was then tuned to the appropriate Larmor frequency followed by aligning the sample (15.11 MHz). The principal axis, or c-axis (c), of the crystal is along the long axis. To begin our measurements, we first aligned c $\perp H_0$. Shown in previous data where $T_1$ was measured with inversion recovery pulses, $T_1^{-1}$ reaches its minimum value when c $\perp H_0$ [9]. Rotating the goniometer in steps of 0.1° or 0.2°, we rotated the goniometer to a minimum $T_1^{-1}$ of 27.845 sec$^{-1}$. To verify this was the correct value, we repeated this process twice and stopped at $T_1^{-1}$ = 30.84 sec$^{-1}$**[Fig 7]**. We denoted this position as $\beta$ = 0°. We recognize a hysteresis when rotating "up" versus "down" and hypothesize it may be from the goniometer setup, however, further investigation is necessary to verify this. $\beta$ Based on previous measurements, we know that the critical field is $B_c$ = 0.515T and we can approach this critical field by rotating the crystal towards a critical angle of $\beta$ = 20° [3]. At each $\beta$, the temperature was increased until the signal became too weak to continue. Spectrum measurements and $T_1$ values were recorded at each temperature. $T_1$ was measured using inversion recovery pulses and fitting the

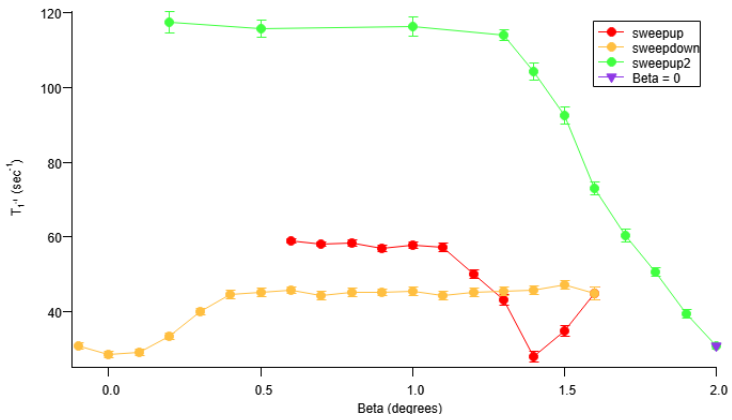


FIG. 7: Each minimum of $T_1^{-1}$ shows us where c $\perp H_0$ occurs. This minimum value was verified twice before starting our measurements.

magnetization recovery to the following expression [10]:

$$M(t) = M_0(1 - f\varphi(t))$$

$$\varphi(s) = 1225/1716e^{28t} + 75/364e^{15t} + 3/44e^{6t} + 1/84e^{t}$$

$B_c$ = $H_0(sin\beta)$

### Discussion

Plotting $1/(T_1T)$ versus temperature, we see peaks where $1/(T_1T)$ is maximum that indicate ferroquadrupolar ordering occurs at some temperature, $T_Q$. $1/T_1$ or $1/T_1T$ usually reaches a maximum at a phase transition due to correlation effects [11]. Our data shows $T_Q$ decreases quickly as the sample rotates further into the c-field **[Fig 8]**. Figure 8 also reveals how it became increasingly difficult to record higher temperatures as $\beta$ increased. The signal to noise (SNR) ratio became too poor to continue past $\beta$ = 5.5°, as indicated with growing error bars. Rather than fitting multiple peaks to calculate $T_1$ as originally planned, we opted for the central peak because it had the highest SNR as we changed the angle and temperature shown in our spectrum plots.

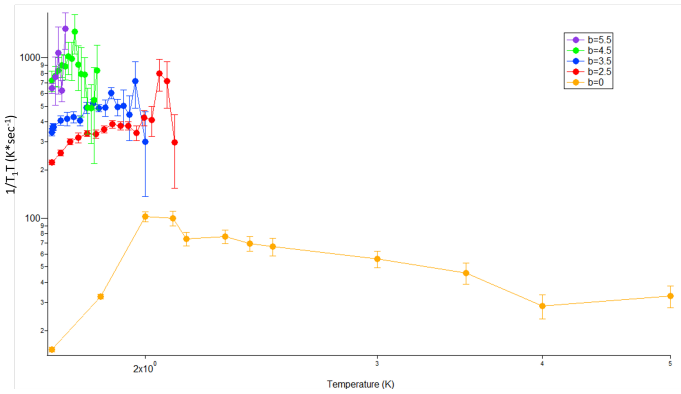


FIG. 8: $1/T_1T$ (K*sec$^{-1}$) plotted as a function of temperature (K) on a log-log scale at each $\beta$. Each angle of rotation was taken to the maximum temperature possible until the signal became too weak for accurate measurements.

Ideally, we would have liked to finish the experiment when $B_c$ = 0.515T at $\beta$ = 20°, however, this was not feasible as our spectrum plots show **[Fig 9]**. The spectrum plots at constant T = 1.7K show seven distinct peaks that quickly deteriorate with noise as the sample rotates **[Fig 9a]**. Likewise, comparing spectrum plots at $\beta$ = 0 the signal also decreases significantly as the temperature increases**[Fig 9b]**. This loss of signal as we increase the temperature or increase beta posed a significant challenge and prevented us from accurately tracking the approach to the QCP. The most likely reason for this behavior is that $T_2$ gets very short near $T_Q$. When $T_2$ is short, the magnetization decays so quickly we cannot measure it (see Eq.(2)). $T_2$ generally gets short near magnetic phase transitions, and it is possible that similar effects are present at the ferroquadrupolar transition in $TmVO_4$ [12]. To compare our

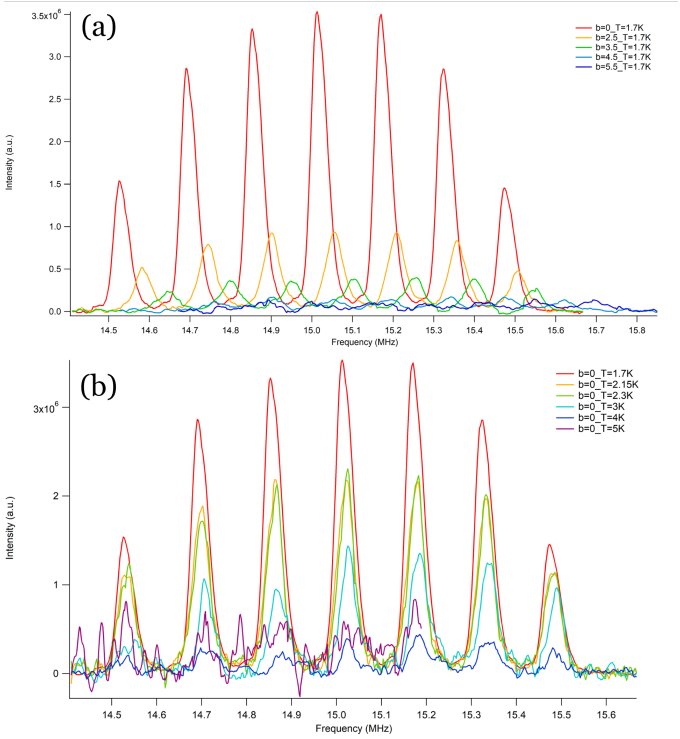


FIG. 9: $TmVO_4$ NMR spectra: (a) constant T = 1.7K, $\beta$ = 0 to $\beta$ = 5.5, (b) constant $\beta$ = 0, T = 1.7K to T = 5K.

data to the reference data in [3], we used a fitting function to accurately determine $T_Q$ from figure 8 that qualitatively reproduces the data and captures the peak in $1/T_1T$ vs T, which is where the phase transition is expected to occur:

if ($t<T_q$)

$$1/(T_1T) = A * t^{\alpha}$$

else

$$1/(T_1T) = A * T_Q^{\alpha} * T_Q/t.$$

Where A is a constant, $\alpha$ is estimated $1/T_1T$, and t is a variable parameter to gauge $T_Q$. The experimental data shows a similar trend of a lower $T_Q$ as $B_c$ approaches the critical field **[Fig 10]**. The deviation from the reference data most likely evolved from the low SNR ratio. Better instrumentation and alterations to the circuit may help resolve this discrepancy.

### Conclusion

In summary, we have performed $^{51}V$ NMR at 1.35T on a polished $TmVO_4$ sample and measured the spectra and spin-relaxation time. We find that $T_Q$ decreases as the sample approaches the critical field, agreeing with previous literature. The loss of signal as T and $\beta$ increase impeded our ability to track the phase transition to higher fields. Moving forward,

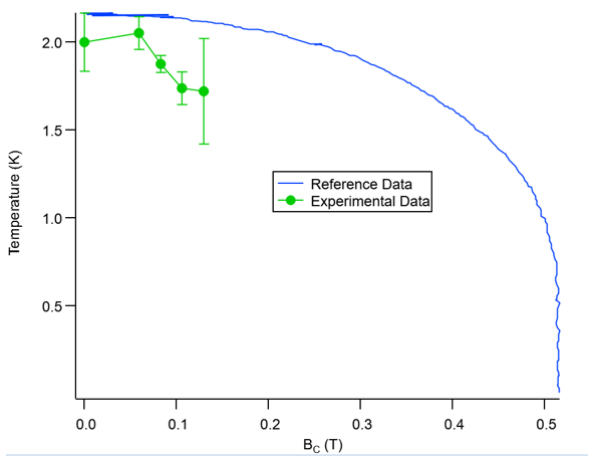


FIG. 10: Critical temperature versus critical field of reference data (blue) and our experimental data (green).

utilizing a Physical Property Measurement System that can reach lower temperatures can help us explore the quantum critical point of this sample. It may also be valuable to measure $T_2$ as a function of temperature to better understand the trends throughout phase space.

**Acknowledgement**

I would like to thank Dr. Nicholas Curro for guidance throughout this project and the opportunity to work in his lab. I would also like to acknowledge Yu-Hsuan Nian, Cameron Chaffey, and Dr. Igor Vinograd for their integral contributions and support. Finally, I would like to thank collaborators at Stanford for their contribution to this project and by providing us with the crystals. Work at UC Davis was supported by the NSF grant PHY-1852581.

[1] Canfield, P. C. Bud'ko, S. L. . Rev., "FeAs-Based Superconductivity: A Case Study of the Effects of Transition Metal Doping on $BaFe_2As_2$," *Rev. Condens. Matter Phys.* **1**, 27 (2010).

[2] Gehring, G.A.; Gehring, "K.A. Co-operative Jahn-Teller effects," *Rep. Prog. Phys.* **1**, 38 (1975).

[3] Proceedings of the Royal Society of London., "K.A. Co-operative Jahn-Teller effects," *Mathematical and Physical Sciences* **Series A, Vol 370**, 131 (1980).

[4] Akash V. Maharaj, Elliott W. Rosenberg, Alexander T. Hristov, Erez Berg, Rafael M. Fernandes, Ian R. Fisher, Steven A. Kivelson., "Transverse fields for Ising-nematic order," *Proceedings of the National Academy of Sciences* **114**, 13430 (2017).

[5] D. Garcia., "Nuclear Magnetic Resonance Spectra of TmVO4," *Physics Department, University of California, Davis*, 1 (2019).

[6] G. M. Wysin wysin@phys.ksu.edu., "Demagnetization Fields," *Department of Physics, Kansas State University*, 1 (2012).

[7] Lars G. Hanson., "Is Quantum Mechanics necessary for understanding Magnetic Resonance?," *Danish Research Centre for Magnetic Resonance Copenhagen University Hospital Hvidovre*, 1 (2019).

[8] Bloch F., "Nuclear induction," *Phys Rev* **70**, 460 (1946)

[9] Z. Wang, I. Vinograd, Z. Mei,1 P. Menegasso, D. Garcia, P. Massat, I. R. Fisher, and N. J. Curro., "Anisotropic nematic fluctuations above the ferroquadrupolar transition in TmVO4 " *Department of Physics, University of California, Davis* **70**, (2021)

[10] Narath, A., "Nuclear Spin-Lattice Relaxation in Hexagonal Transition Metals: Titanium" *Phys. Rev., American Physical Society* **162**, 320 (1967)

[11] Curro, N. J. Avella, A. Mancini, F. (Eds.)., "Nuclear Magnetic Resonance as a Probe of Strongly Correlated Electron Systems" *Springer*, 1 (2014)

[12] Curro, N.; Hammel, P.; Pagliuso, P.; Sarrao, J.; Thompson, J. Fisk, Z.., "Evidence for spiral magnetic order in the heavy fermion material $CeRhIn_5$ " *Phys. Rev. B* **62**, (2000)